Calcification Transformation Process of High-Iron Red Mud for Sustainable Alumina Production

Xin He [1], Guo-zhi Lv[2], Zhuang-zhuang Yun[3], Qing-dong Li[4] and Ting-an Zhang[5]
1, 3, 4. PhD students
2, 5. Professors
School of Metallurgy – Northeastern University, Shenyang, China
Corresponding author: lvgz@smm.neu.edu.cn
https://doi.org/10.71659/icsoba2025-br010

Abstract

The Bayer process is the predominant process for global alumina production, resulting in the generation of a significant volume of highly alkaline red mud. The absence of cost-effective treatment techniques has led to the stockpiling of most red mud, which poses a serious ecological threat due to its high alkalinity. This paper addresses the global challenge of red mud generated from alumina production by proposing a novel approach for its low-cost and large-scale utilization, focusing on mineral phase reconstruction and high-value end products. A new technology, the "calcification-transformation" process, has been developed based on the leaching characteristics of the Bayer process and the mineral structure of red mud. This process can effectively utilize red mud and facilitate the synergistic extraction of valuable elements contained within it. A comprehensive investigation has been conducted to examine how various parameters of the calcification-transformation process influence its effectiveness. Utilizing X-ray fluorescence (XRF), X-ray diffraction (XRD), and scanning electron microscopy (SEM), the chemical compositions, phase compositions, and microstructures of red mud and the slag produced at each stage of the calcification-transformation process were analyzed. The results indicate that temperature and the calcium-to-silicon ratio significantly affect the calcification process. Specifically, at a calcination temperature of 260 °C, with a calcium-to-silicon ratio of 2, a caustic soda concentration of 230 g/L, a molecular ratio of sodium aluminate solution, a liquid-to-solid ratio of 4:1, and a reaction time of 60 minutes, the Na_2O and A/S in the calcined slag were found to be 0.61 % and 1, respectively. The transformed slag can be utilized to produce iron-making pellets, providing high-quality raw materials for the steel industry. This process not only reduces the demand for iron ore mining but also promotes the comprehensive utilization of red mud. This technology is essential for alleviating existing red mud stockpiles and fostering sustainable alumina production within the industry.

Keywords: Environmentally friendly, Red mud, Calcification transformation, Complete treatment, Mine phase reconstruction.

1. Introduction

Red mud (also called bauxite residue) is a highly alkaline solid waste produced during the alumina extraction process [1, 2]. The quantity of red mud generated varies based on the source, grade, and processing methods of bauxite, typically ranging from 1.5 to 2.5 tonnes per tonne of alumina produced [3]. In recent years, the rapid expansion of the alumina industry has led to an increase in the volume of red mud discharged [4]. Currently, the global stockpile of red mud exceeds 4 Gt and continues to grow at a rate of 180 Mt annually. Notably, China's red mud stockpile has surpassed 600 Mt. The global average utilization rate of red mud stands at 15 %, while in China, this rate is only 4 % [5]. At present, red mud is primarily managed through the dry stacking method, which not only causes infiltration and pollution of surface and groundwater but also contaminates the air and soil, posing significant hazards to the surrounding environment and wildlife, and creating safety risks [1, 6, 7]. The 2010 collapse of the red mud dam at the Ajka

alumina plant in Hungary resulted in ten fatalities include three missing persons, with the highly alkaline red mud severely impacting several European countries along the Danube River. This incident served as a wake-up call for the alumina industry worldwide [8].

Red mud can be categorized based on the production process into three types: sintering process red mud, Bayer process red mud, and combined process red mud [9]. The Bayer process accounts for over 90 % of global alumina production [10]. The primary chemical components found in red mud include Al_2O_3, SiO_2, Fe_2O_3, CaO, TiO_2, Na_2O, and MgO, along with trace elements such as K, Ga, Mn, Ni, V, and rare earth elements [11]. The concentration of these main chemical components varies among different types of red mud, influenced by the alumina production processes and the raw materials sourced from bauxite ore [12]. Table 1 below illustrates the composition of red mud derived from various processes and origins. Notably, red mud produced by the Bayer process exhibits higher concentrations of Na_2O, Al_2O_3, and Fe_2O_3 when compared to that from the sintering or combined processes. In contrast, red mud from the sintering or combined processes typically shows elevated levels of SiO_2 and CaO relative to the Bayer process.

Table 1. Comparison of main components of typical Bayer process red mud, sintering process red mud, and combined process red mud (wt%).

Method	**Bayer process**			**Sintering method**			**Combined process**	
Location	Gui Zhou	Guang Xi	Queensland	Gui Zhou	Shan Dong	Shan Xi	He Nan	Shan Xi
Na_2O	4.0	4.0	4–10	3.1	2.8	2.60	2.58–3.68	2.6–3.4
Al_2O_3	32.0	17.47	15–20	8.5	6.4	8.22	5.96–8	8.2–12.8
SiO_2	12.8	11.93	24–29	25.9	22.00	21.43	18.9–20.7	21.4–23
CaO	22.0	14.13	0.5–4	38.4	41.90	46.80	39–43.3	37.7–46.8
Fe_2O_3	3.4	32.47	21–36	5.0	9.02	8.12	10–12.6	5.4–8.1
MgO	3.9	-	0.5–1	1.5	1.70	2.03	2.15–2.6	2.0–2.9
K_2O	0.2	1.0	-	0.2	0.30	0.20	0.47–0.59	0.2–1.5
TiO_2	6.5	5.45	-	4.4	3.20	2.90	6.13–6.7	2.2–2.9
LOI	10.7	9.46	7–12	11.1	11.70	8.00	6.5–8.15	8.0–12.8
Others	4.5	4.09	-	1.9	0.98	-	-	-

The iron content in red mud generated from the Bayer process for alumina production is typically high, with some samples exceeding 30 % total iron content. The combined content of Fe_2O_3 and Al_2O_3 can reach as high as 50 %, positioning red mud as a valuable secondary resource for iron and aluminum [13]. The recovery and utilization of valuable metals, such as iron and aluminum, represent significant pathways for the resource utilization of high-iron red mud [12]. Extensive research has been conducted both domestically and internationally on the recovery of iron from high-iron red mud, primarily utilizing physical separation methods [14], hydrometallurgical recovery [15], and pyrometallurgical recovery [16]. While physical separation methods are straightforward and easy to operate, they yield a low iron recovery rate and produce iron concentrates of low grade （TFe < 50%） [17]. The impurities present in red mud consume substantial amounts of acid during the hydrometallurgical recovery process, which not only increases the cost of iron extraction but also contributes to secondary pollution through the generation of considerable waste liquid [18]. Pyrometallurgical recovery of iron involves the

direct reduction of hematite using a reducing agent to ultimately obtain metallic iron. Although this method exhibits high recovery efficiency, its industrial application is limited due to high energy consumption and the alkaline content of red mud, which presents challenges to the alkali load of blast furnaces [19].

To address the issue of red mud accumulation, dealkalization is crucial. The global challenge posed by Bayer process red mud stems from the equilibrium solid phase associated with its dissolution: sodium aluminosilicate hydrate $Na_2O{\cdot}Al_2O_3{\cdot}1.7SiO_2{\cdot}nH_2O$ (where $n \leq 2$). In this phase, the mass ratio of Al_2O_3 to SiO_2 is approximately 1:1, while the sodium oxide-to-silica ratio is about 0.608:1. Consequently, for every unit mass of silica, there is an inevitable loss of one unit mass of alumina and 0.6 unit mass of sodium oxide. To effectively address the limitations of the Bayer process, it is essential to disrupt the structure of the equilibrium solid phase during dissolution and develop a new structure for red mud. Additionally, it is essential to consider the costs and challenges associated with scaling up the technology for industrial implementation [20]. This involves managing the complexity of process reactions and equipment costs to achieve the lowest possible expenditure while ensuring the efficient recovery of valuable components from red mud. Considering this, the present study proposes a comprehensive red mud utilization technology focused on high-value end-product applications. This technology enhances the dissolution of alumina and the recovery of caustic alkali from red mud through high-temperature calcification, ultimately resulting in a novel red mud structure that is nearly free of alkali. This product can be directly utilized as a raw material in iron ore pellet production, thereby circumventing the complications associated with high alkali content in blast furnaces. Furthermore, the study thoroughly investigates the effects of process parameters, including temperature, calcium-to-silicon ratio, caustic alkali concentration, and time, on the efficiency of calcification transformation. The phase analysis of high-iron red mud transformation slag was performed using X-ray diffraction. The innovative application of steel-aluminum collaboration not only offers a viable solution for red mud disposal but also provides high-quality raw materials for blast furnace steelmaking.

2. Experimental

2.1 Materials

The red mud utilized in this experiment was obtained from an alumina plant located in Shandong Province, China. This red mud is a byproduct of the Bayer process for the dissolution of gibbsite ore. The chemical composition of the red mud is detailed in Table 2. Notably, the combined content of iron and aluminum in the red mud exceeds 60 %, with an exceptionally high iron content. The total iron grade approaches 40 %, and the aluminum-to-silicon ratio exceeds 3, indicating that it is a valuable secondary resource for iron and aluminum. Figure 2 illustrates the XRD pattern of this red mud, revealing the presence of key phases such as hematite (Fe_2O_3), sodalite ($1.08Na_2O{\cdot}Al_2O_3{\cdot}1.68SiO_2{\cdot}1.68H_2O$), anatase ($Fe_2O_3$), boehmite (AlO(OH)), silicon dioxide (SiO_2), and goethite (FeO(OH)).

Table 2. Chemical composition of high-iron red mud (wt%).

Na_2O	Al_2O_3	SiO_2	CaO	TiO_2	TFe	A/S
2.58	23.4	7.62	2.25	6.06	39.55	3.07

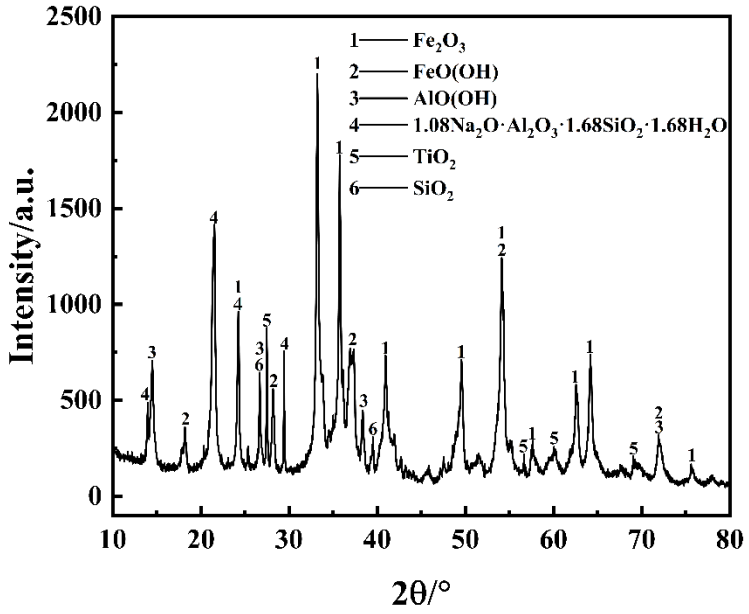

Figure 1. The XRD pattern of high-iron red mud.

2.2 Methods

As illustrated in Figure 2, the calcification transformation stage represents a hydrometallurgical process. The raw materials for the reaction, which include high-iron red mud, calcium oxide, and sodium aluminate solution, are introduced into a high-pressure reactor in a precise ratio. Experimental parameters such as reaction temperature and stirring speed are controlled via the control panel. Once the experiment commences, cooling water is continuously supplied to the stirring paddle to prevent motor overheating. The timing begins when the reaction temperature reaches the specified experimental conditions. After the designated reaction time has elapsed, the heating jacket is removed, and cooling water is introduced to lower the reactor body temperature. Once the temperature has cooled to room temperature, the gas valve is opened to reduce the internal pressure to 0 MPa, allowing for the safe opening of the reactor. Subsequently, the transformed red mud slurry is discharged, and solid-liquid separation is carried out using a vacuum circulating water pump-type filter, followed by alkali removal through water washing. The solid phase is retained and placed in a blast drying oven for drying. Finally, the transformed reduction slag undergoes testing.

Under optimal reaction conditions, the calcined transformation slag is mixed with an appropriate amount of binder and magnetite. Small balls, measuring 10 to 16 mm, are then prepared using a disc pelletizer and subsequently dried at low temperatures. The dried green pellets are heated in a vertical resistance furnace at a rate of 10 °C per minute until they reach 900 °C, where they are held for 60 minutes. Following this, the temperature is increased directly to 1250 °C and maintained for an additional 30 minutes before the pellets are cooled to room temperature within the resistance furnace.

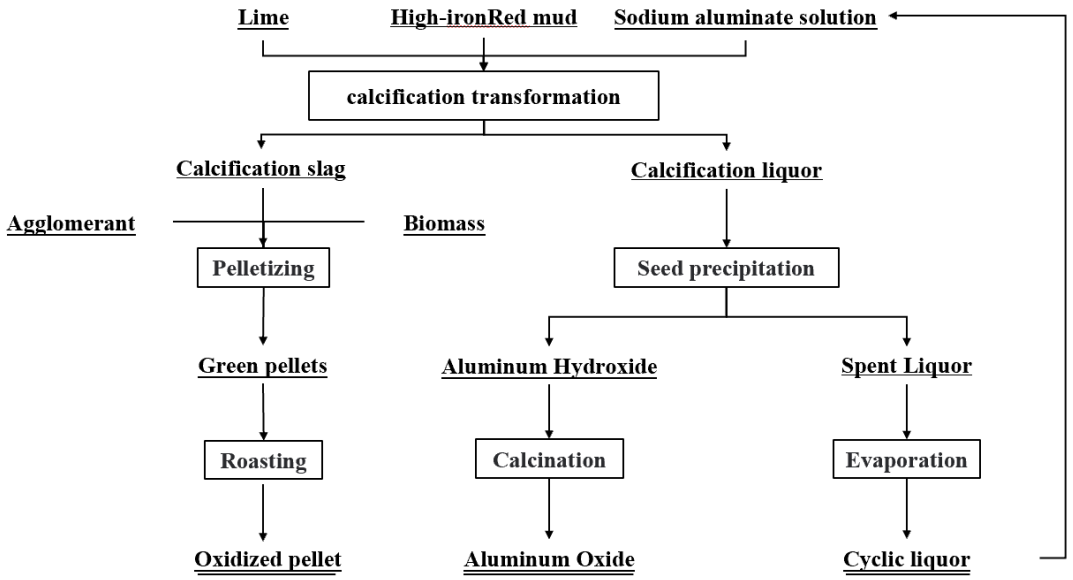

Figure 2. The flowchart of the calcification transformation process.

The recovery rate of alumina could be calculated by Equation (1).

$$\eta_{Al} = \frac{(A/S)_O - (A/S)_R}{(A/S)_O} \times 100\ \% \quad (1)$$

Where:
η_{Al} actual extraction rate of Al_2O_3, %
$(A/S)_O$ mass ratio of Al_2O_3 to SiO_2 in bauxite
$(A/S)_R$ mass ratio of Al_2O_3 to SiO_2 in red mud.

2.3 Characterization

The chemical composition of the transformed residue from the calcification process was quantitatively analyzed using the glass fusion method on an X-ray fluorescence spectrometer (ZSX Primus IV). The phase composition of both the bauxite raw material and the transformed red mud was analyzed using X-ray diffraction (XRD) with a D8 Advance instrument (Bruker, Germany) operating at 40 kV and 40 mA.

3. Results and Discussion

3.1 Effect of Calcification Transformation Parameters

3.1.1 Effect of Temperature

This study investigates the effect of temperature on the calcification reaction by maintaining a sodium oxide concentration (Na_2O) of 210 g/L, a calcium-to-silicon molar ratio of 2, a liquid-to-solid ratio of 4:1, a stirring speed of 300 rpm, and a transformation time of 60 minutes. The aim is to evaluate the impact of temperature on the calcification transformation efficiency of red mud. The experimental results are presented in Figure 3. As illustrated in Figure 3, at a reaction temperature of 240 °C, the sodium oxide content in the red mud decreased to 1.07 %, while the alumina recovery rate reached 66.38 %. This indicates that the calcification transformation significantly reduced the sodium content in the red mud and enhanced the dissolution of residual

alumina. When the temperature was increased from 240 °C to 260 °C, the sodium oxide content further decreased from 1.07 % to 0.61 %, and the alumina recovery rate increased to 67.31 %. However, with continued increases in temperature, both the sodium oxide content in the red mud and the leaching rate of alumina exhibited minimal changes. Considering energy consumption, 260 °C was determined to be the optimal reaction temperature.

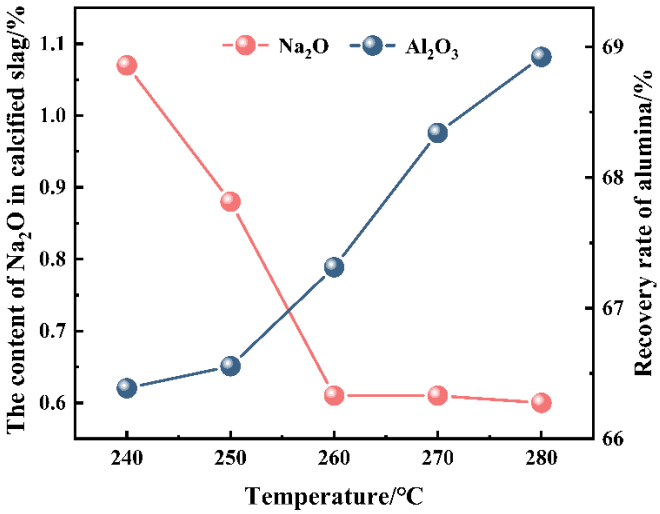

Figure 3. Effect of temperature on the recovery rate of alumina and the content of Na_2O in calcified slag.

3.1.2 Effect of Molar Ratio of CaO to SiO_2

The amount of calcium oxide added plays a crucial role in the calcium transformation process of red mud. With the reaction temperature fixed at 260 °C, sodium oxide (Na_2O) concentration at 210 g/L, a liquid-to-solid ratio of 4:1, stirring speed at 300 rpm, and a transformation time of 60 minutes, we investigated the effect of the molar ratio of CaO to SiO_2 (C/S) on the calcium transformation, as illustrated in Figure 4. As shown in Figure 4, an increase in the amount of calcium oxide leads to a gradual decrease in the residual Na_2O content in the calcium-transformed red mud. Specifically, when the calcium-to-silicon molar ratio reaches 2, the residual Na_2O content drops to 0.61 %. However, as the calcium-to-silicon ratio continues to rise, the residual Na_2O content in the red mud remains relatively stable, exhibiting a slight upward trend. Furthermore, the alumina extraction rate during the calcification transformation process decreases as the calcium-to-silicon molar ratio increases. This phenomenon occurs because the silicon saturation coefficient of hydrogarnet ($Ca_3Al_2(SiO_4)(OH)_8$) is lower than that of sodalite, leading to a greater proportion of alumina entering the hydrogarnet and resulting in alumina loss. It is important to note that increasing the calcium oxide content cannot eliminate the residual Na_2O content in the red mud completely. The essence of the calcification transformation process involves the conversion of hydrated sodium aluminosilicate (including sodalite and cancrinite) in the red mud into hydrogarnet. Throughout the reaction and extraction process, a certain equilibrium is maintained between hydrated sodium aluminosilicate and hydrogarnet. Therefore, merely increasing the calcium-to-silica ratio cannot entirely remove the alkali from the red mud. When excessive amounts of CaO are added, the surplus calcium oxide reacts with aluminum or silicon to form hydrated calcium aluminate or hydrated calcium silicate compounds, which negatively impacts the recovery of alumina. Consequently, it is essential to establish a balance in the calcification transformation process to reduce sodium oxide in red mud while minimizing the loss of caustic alkali in hydrogarnet. Thus, a calcium-to-silica molar ratio of 2 is identified as the optimal ratio, at which the sodium oxide content in the transformed red mud is 0.61 %, and the alumina recovery rate is 67.31 %.

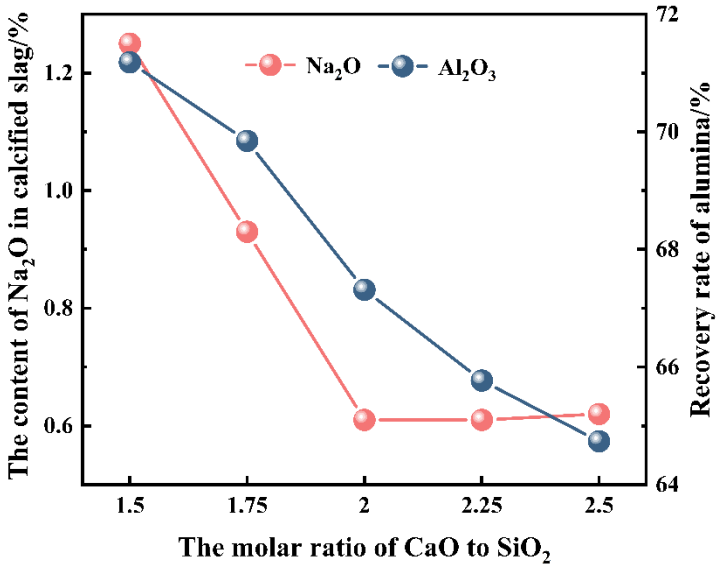

Figure 4. Effect of the molar ratio of CaO to SiO_2 on the recovery rate of alumina and the content of Na_2O in calcified slag.

3.1.3 Effect of Na_2O concentration

The reaction temperature was maintained at 260 °C, with a calcium-to-silicon molar ratio of 2, a liquid-to-solid ratio of 4:1, a stirring speed of 300 rpm, and a reaction time of 60 minutes. The influence of sodium oxide concentration on the yield of alumina ($\eta(Al_2O_3)$) and the sodium oxide content in the calcified slag was investigated, with the results illustrated in Figure 5. As shown in Figure 5, an increase in the concentration of caustic alkali in the sodium aluminate solution correlates with a decrease in both the sodium oxide content in the calcified slag and the leaching rate of alumina.

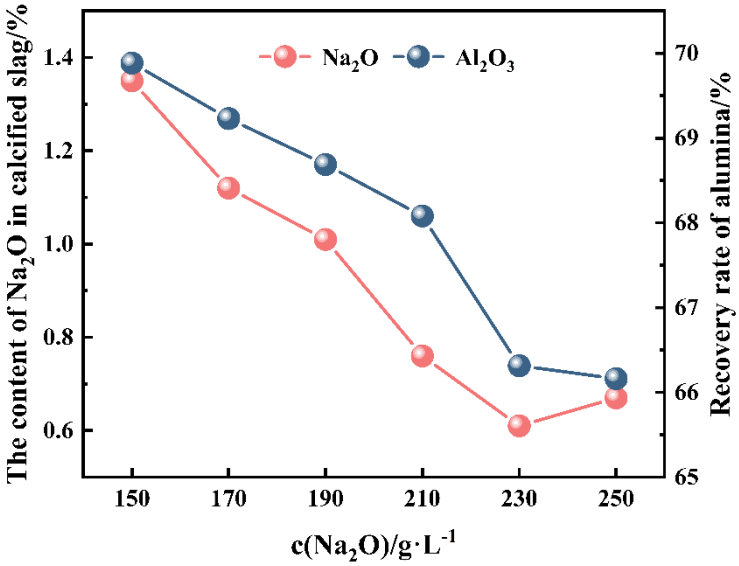

Figure 5. Effect of Na_2O concentration on the recovery rate of alumina and the content of Na_2O in calcified slag.

This indicates that an appropriate increase in caustic alkali concentration in sodium aluminate is advantageous for facilitating the calcification transformation reaction. At a caustic alkali

concentration of 230 g/L, the sodium oxide content in the transformation residue is 0.61 %, and the alumina recovery rate from red mud is 67.31 %. However, further increases in caustic alkali concentration may lead to heightened system viscosity, which can impede mass transfer during the reaction. Consequently, a concentration of 230 g/L is identified as the optimal level of caustic alkali.

3.1.4 Effect of Time

The fixed reaction temperature is set at 260 °C, with a calcium-to-silicon molar ratio of 2, a liquid-to-solid ratio of 4:1, a stirring speed of 300 rpm, and a Na_2O concentration of 210 g/L. This study investigates the effects of reaction time on the concentration of Na_2O in the calcified slag and the recovery rate of Al_2O_3, as illustrated in Figure 6. As shown in Figure. 6, at a reaction time of 15 minutes, the Na_2O content in the calcified slag is 1.33 %, and the recovery rate of Al_2O_3 is 69.56 %. However, as the reaction time increases, both the Na_2O content in the calcified slag and the recovery rate of Al_2O_3 exhibit a decreasing trend. This phenomenon may be attributed to the kinetic control of the hydrogarnet formation process. In the initial reaction phase, undissolved boehmite in the red mud quickly dissolves into the solution while the formation of the hydrogarnet phase begins. As the reaction progresses, an increasing amount of sodalite in the red mud gradually transforms into hydrogarnet due to the influence of calcium oxide. Since the silicon saturation coefficient of hydrogarnet is slightly higher than that of sodalite, this results in a partial loss of alumina within the hydrogarnet phase, leading to a decrease in the recovery rate of alumina. Therefore, it is essential to balance the remaining sodium oxide in the red mud to minimize alumina loss without compromising the subsequent utilization of red mud. At a reaction time of 60 minutes, the sodium oxide content in the calcified slag is 0.61 %, and the recovery rate of alumina from the red mud is 67.31 %.

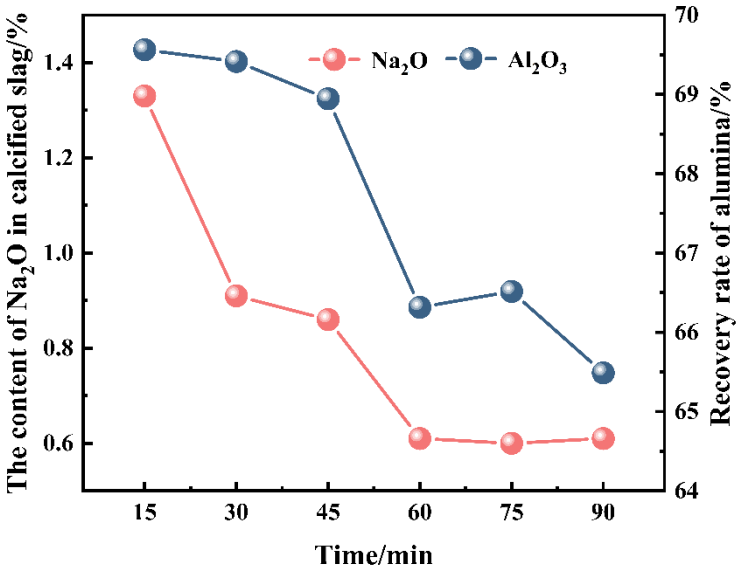

Figure 6. Effect of time on the recovery rate of alumina and the content of Na_2O in calcified slag.

3.2 XRD of Calcified Slag

To clarify the phase composition of the transformed red mud following calcium transformation, the reaction conditions were set as follows: a temperature of 260 °C, a sodium oxide concentration of 210 g/L, a molar ratio of calcium to silicon of 2, a liquid-to-solid ratio of 4:1, and a reaction time of 60 minutes. The X-ray diffraction (XRD) analysis of the calcium transformation residue is presented in Figure 7. As illustrated in Figure 7, all characteristic diffraction peaks of the

sodium-containing phase, sodalite, in the red mud disappeared after the calcium transformation and leaching. Conversely, new characteristic diffraction peaks of hydrogarnet emerged in the transformation residue, while hematite did not participate in the reaction during the transformation and leaching process, remaining present in the transformed red mud. The primary phases in the final calcium residue are hydrogarnet ($Ca_3Al_2(SiO_4)(OH)_8$) and hematite (Fe_2O_3).

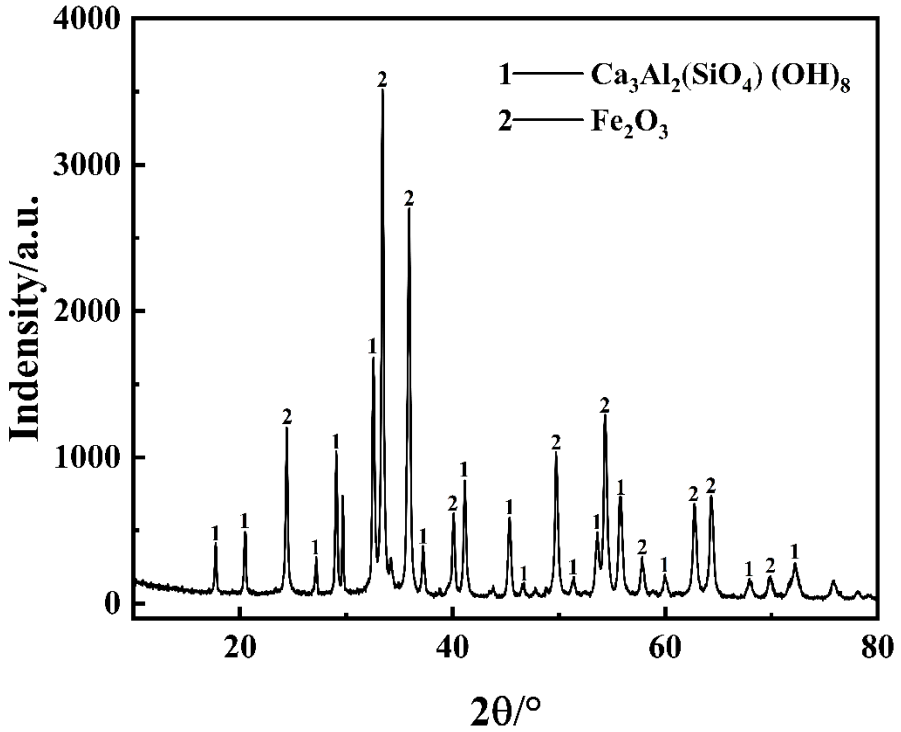

Figure 7. The XRD pattern of calcified slag.

3.3 Complete Utilization of Calcified Transformation Red Mud

With the development of the steel industry, the easily minable high-grade iron ores are gradually depleting, making the mining and utilization of low-grade iron ores an inevitable trend. The red mud, which has been transformed through calcification, still contains abundant iron resources (TFe > 35 %). To achieve high-value utilization and complete consumption of calcified red mud, this technology proposes a novel approach: aluminum-iron co-smelting. The low-alkali red mud, after calcification, is used as a raw material and blended with iron concentrate in varying proportions of calcification slag to prepare ironmaking pellets. Due to its low alkalinity, it does not affect the alkali load of the blast furnace. The composition and properties of the roasted pellets are presented in Table 3. As indicated in Table 3, the oxidized pellets prepared from calcified red mud, although the total iron content is slightly lower than the pellet ore standard, exhibit a compressive strength exceeding 2000 N. Furthermore, their impurity composition and strength properties fully meet the requirements for pellets used in blast furnace ironmaking. The total iron content of the pellets can be adjusted to comply with national standards (TFe > 65 %) by reducing the amount of red mud added. Therefore, calcified red mud can be utilized as a high-quality iron-containing resource to produce ironmaking pellets, facilitating not only the clean production of alumina but also ensuring the iron ore reserves.

Table 3. Composition and properties of pellets prepared from calcined slag.

addition of calcined slag	Na_2O	Al_2O_3	SiO_2	CaO	Fe_2O_3	SO_3	P	Compressive strength
35 %	0.51	1.5	2.94	4.29	76.69	0.11	0.032	2631 N

4. Conclusions

Addressing the challenge of limited low-cost and large-scale disposal methods for high-iron red mud, primarily due to its elevated alkali content, this study introduces a novel high-temperature calcification process that leverages mineral phase reconstruction. This innovative approach not only facilitates the efficient recovery of sodium oxide and alumina but also ensures the complete disposal of red mud. The dissolution of undissolved boehmite in red mud can be improved during the calcification transformation process. Under the specified conditions of a reaction temperature of 260 °C, a calcium to silicon molar ratio of 2, a liquid to solid ratio of 4:1, a stirring speed of 300 rpm, a sodium oxide concentration of 210 g/L, and a reaction time of 60 minutes, the sodium oxide content in the calcification slag was found to be 0.61 %, while the alumina recovery rate reached 67.31 %. These findings indicate that the calcification transformation process yielded favorable results.

During the calcification transformation process of high-iron red mud treatment, the sodium-containing phase (sodalite) in the slag, gradually converts into an alkali-free hydrogarnet phase under low-temperature conditions. In contrast, the iron-containing phase in the red mud persists in the calcification transformation slag as hematite.

As a result of its low alkalinity, the calcification-transformed red mud is a particularly valuable iron containing resource. By incorporating 35 % calcification slag and following a suitable batching and pelletizing process, the resulting pellets exhibit impurity composition and strength properties that comply with the standards for ironmaking pellets.

5. Declaration of Competing Interest

The authors declare that they have no known competing financial interests or personal relationships that could have appeared to influence the work reported in this paper.

6. Data Availability

Data will be made available on request.

7. Acknowledgments

This work was financially supported by the National Natural Science Foundation of China (No. ZX20230386), the 2023 Special Project for High-Industrial Base Reconstruction Quality Development of the Manufacturing Industry (No. 2023ZY01019–11), the Jiangxi Province “Double Thousand Plan” Project (No. S2021DQKJ2198), and the sixth batch of top talent support funds (No. QNBJ-2022-04).

8. References

1. R.B. Meshram, et al., Recovery of valuable metals from red mud: a review on leaching and separation processes, *Discover Applied Sciences*, 6(10), 2024, 537. https://doi.org/10.1007/s42452-024-06253-x
2. É. Ujaczki, et al., Red mud valorisation using bioleaching: a review, *Journal of Chemical Technology and Biotechnology*, 92(10), 2017, 2683–2690. https://doi.org/10.1002/jctb.5289
3. X. Liu, et al., Recovery of scandium from red mud leachate using solvent extraction with d2ehpa, *Environmental Science and Pollution Research*, 30(15), 2023, 43377–43386. https://doi.org/10.1007/s11356-023-25389-8
4. N.C.G. Silveira, et al., Sustainability analysis of red mud management in Brazil, *Sustainability*, 13(22), 2021, 12741. https://doi.org/10.3390/su132212741

5. T. Zhang, et al., Recovery of rare earth elements from red mud by integrated process, *Light Metals* 2018, 135–141.
6. S. Abhishek, A. Ghosh, B. Pandey, A review on red mud valorization: challenges and opportunities in metal recovery and environmental management, *Environmental Science and Pollution Research*, 2024, https://doi.org/10.1007/s11356-024-35217-2
7. X. Yang, et al., Two-factor authentication for intellectual property transactions based on improved zero-knowledge proof, *Scientific Reports*, 15, 2025, 7255. https://doi.org/10.1038/s41598-025-90570-7
8. A. Gelencsér, et al., Atmospheric aging of red mud aerosol: formation of respirable secondary particles, *Environmental Science and Technology*, 45(4), 2011, 1608–1615. https://doi.org/10.1021/es104005r
9. Y. Xiao, et al., A review on the utilization of red mud as sustainable construction materials, *Journal of Zhejiang University - Science A*, 23(5), 2022, 335–357. https://doi.org/10.1631/jzus.A2100476
10. D. Brough, H. Jouhara, The aluminium industry: a review on state-of-the-art technologies, environmental impacts and possibilities for waste heat recovery, *International Journal of Thermofluids*, 1–2, 2020, 100007. https://doi.org/10.1016/j.ijft.2019.100007
11. P. Wang, D.-Y. Liu, Red mud and its utilization in cementitious materials, *Materials (Basel)*, 5(10), 2012, 1800–1810. https://doi.org/10.3390/ma5101800
12. K. Wang, et al., Recovery of scandium from red mud using acid leaching and solvent extraction, *Environmental Science and Pollution Research*, 29(60), 2022, 89834–89852. https://doi.org/10.1007/s11356-022-23837-5
13. Q. Li, et al., Summary of research progress on the separation and extraction of iron from bayer red mud, *Journal of Sustainable Metallurgy*, 11(1), 2025, 186–213. https://doi.org/10.1007/s40831-024-00986-0
14. S. Rai, et al., Recovery of rare earth elements from red mud leach liquor using solvent extraction, *Minerals Engineering*, 134, 2019, 222–231. https://doi.org/10.1016/j.mineng.2019.02.018
15. Y. Yang, et al., Recovery of scandium from red mud by acid leaching and solvent extraction, *Hydrometallurgy*, 157, 2015, 239–245. https://doi.org/10.1016/j.hydromet.2015.08.021
16. J. Xiao, et al., An efficient process to recover iron from bayer red mud, *JOM*, 74(8), 2022, 3172–3180. https://doi.org/10.1007/s11837-022-05373-2
17. G. Lu, et al., Recovery of rare earth elements from red mud by acid leaching and precipitation, *Hydrometallurgy*, 188, 2019, 248–255. https://doi.org/10.1016/j.hydromet.2019.05.018
18. G. Pilla, et al., Sustainable valorization of bauxite residue through thermal treatment and material recovery, *Sustainable Materials and Technologies*, 43, 2025, e01289. https://doi.org/10.1016/j.susmat.2025.e01289
19. H. Fu, et al., Study on iron extraction from high iron bauxite residue by pyrite reduction, *Bulletin of Environmental Contamination and Toxicology*, 109(1), 2022, 149–154. https://doi.org/10.1007/s00128-022-03520-8
20. H. Zeng, et al., Recovery of valuable metals from red mud by carbothermic reduction and magnetic separation, *JOM*, 72(1), 2020, 319–325. https://doi.org/10.1007/s11837-019-03911-z